The Influence of Water on the Nanomechanical Behavior of the Plant Biopolyester Cutin as Studied by AFM and Solid-State NMR

Andrew N. Round, Bin Yan, Soa Dang, Racha Estephan, Ruth E. Stark, and James D. Batteas
Department of Chemistry, The City University of New York, College of Staten Island and The Graduate Center, Staten Island, New York 10314-6609 USA

ABSTRACT Atomic force microscopy and solid-state nuclear magnetic resonance have been used to investigate the effect of water absorption on the nanoscale elastic properties of the biopolyester, cutin, isolated from tomato fruit cuticle. Changes in the humidity and temperature at which fruits are grown or stored can affect the plant surface (cuticle) and modify its susceptibility to pathogenic attack by altering the cuticle's rheological properties. In this work, atomic force microscopy measurements of the surface mechanical properties of isolated plant cutin have been made as a first step to probing the impact of water uptake from the environment on surface flexibility. A dramatic decrease in surface elastic modulus (from ~32 to ~6 MPa) accompanies increases in water content as small as 2 wt %. Complementary solid-state nuclear magnetic resonance measurements reveal enhanced local mobility of the acyl chain segments with increasing water content, even at molecular sites remote from the covalent cross-links that are likely to play a crucial role in cutin's elastic properties.

INTRODUCTION

The aerial surfaces of the leaves and fruits of higher plants consist of a cuticular membrane that occupies approximately 100 nm to 20 μm of the outer covering (Walton, 1990). The membrane is composed of a variety of waxes ($\sim C_{30}$ aliphatic lipids) for waterproofing and an insoluble biopolyester, cutin (cross-linked hydroxy- and epoxy-fatty acids), which serves as a dense networked structural support. Typically, thin layers of epicuticular lipids coat the outer surface of the cuticle. Additionally, intracuticular lipids (predominantly fatty acids) are embedded within the cutin matrix. The specifics of plant cuticular composition have been investigated and reviewed (Kolattukudy, 1980, 1984; Holloway, 1982; Baker, 1982; Walton, 1990).

The cuticular membrane plays many roles in the survivability of the plant. It functions as a barrier to protect leaves and fruit from the environment and from pathogenic attack. The cuticle also controls the diffusion of molecules into plant tissues and prevents water loss. Finally, the cuticular surface composition and structure control the wettability of the plant by agriculturally important chemicals. The attack and breakdown of this barrier by bacterial and fungal pathogens has been associated with an estimated $10 billion loss due to crop damage in the United States (Agrios, 1988). Chemical, thermal, and mechanical stresses can all promote fracturing of the cuticle, seriously compromising its protective functions. In order to understand and design approaches to augment cuticular integrity, it is therefore important to characterize such properties as surface morphology and elasticity as a function of environmental variables and to link them with molecular structure.

Cuticular ultrastructure has been investigated extensively with transmission and scanning electron microscopies (Kolattukudy, 1980, 1984; Holloway, 1982; Baker, 1982). The development of the atomic force microscope (AFM) has enabled the direct examination of the three-dimensional architecture of biological surfaces, including plant tissues and surfaces (Gould et al., 1990; Canet et al., 1996; Kirby et al., 1996; Mechaber et al., 1996; Round et al., 1996), with spatial resolutions at or near those of electron microscopies, under ambient gas or liquid environments and with little or no special preparation of the samples. Thus AFM provides the opportunity for nanometer-scale, non-intrusive, three-dimensional imaging of surface structure under ambient environmental circumstances.

Because of the cuticle's barrier role, its rheology is of particular interest. The cuticle can be modeled as a viscoelastic polymer network, as has been demonstrated by recent stress-strain studies (Petracek and Bukovac, 1995). Factors that affect the rheological properties of the cuticle, such as plasticizing by water, can also influence its permeability, an important consideration if foliar applied chemicals are to be used agriculturally. It has been proposed (Garbow and Stark, 1990) that insufficient flexibility of the cuticle may promote cracks in the polymeric veneer, making the underlying tissue susceptible to pathogenic attack. Despite the importance of cuticular mechanical response to the environment, to our knowledge only a single study of cuticular rheology has been performed (Petracek and Bukovac, 1995). With the advent of AFM as a probe of surface nanomechanical behavior (Domke and Radmacher, 1998; Gracias and Somorjai, 1998; Kiridena et al., 1997; Laney et al., 1997; Overney et al., 1994; Radmacher et al., 1992), the effect of environmental or solvent changes on the cuticle's surface rheological behavior can be probed at the nanometer scale. Nanomechanical measurements made by AFM in-

Received for publication 1 October 1999 and in final form 31 July 2000.
Address reprint requests to James D. Batteas, Department of Chemistry, The City University of New York, College of Staten Island and The Graduate Center, 2800 Victory Boulevard, Staten Island, NY 10314-6609. Tel.: 718-982-4075; Fax: 718-982-3910; E-mail: batteas@postbox.csi.cuny.edu.

0006-3495/00/11/2761/07 $2.00

volve controlling the force with which the AFM probe is pressed against a sample material. The resulting plot of force versus distance from the sample surface contains information about local rheological properties such as elasticity and adhesion. This information may be extracted from the theoretical framework of continuum contact mechanics constructed by, among others, Hertz (1882) and the group of Johnson, Kendall, and Roberts (Israelachvili, 1985; Johnson, 1985). The use of AFM in this way has become more widespread in recent years, because it provides unrivaled data on the surface mechanical properties of a material in cases where surface conditions may be very different from those sensed by a bulk measurement.

Here we present the first AFM studies of the biopolyester cutin, isolated from the cuticle of tomato fruit *(Lycopersicon esculentum*) as a probe of the surface elastic modulus in response to changes in humidity, an important consideration in that the tomato's ubiquity means that it is grown under a broad range of conditions. We elected to isolate cutin from tomato fruit cuticle as a model system for plant fruit surfaces because it has a simple composition, i.e., it is derived almost exclusively (>93%) from a single monomeric component, 10,16-dihydroxyhexadecanoic acid (Gerard et al., 1992). In a complementary fashion, cross-polarization magic-angle spinning ^{13}C nuclear magnetic resonance (CPMAS NMR) has been used to obtain molecular-scale structural and dynamic information on bulk solid samples of plant cuticle. For instance, $T_1(C)$ and $T_{1\rho}(C)$ relaxation experiments have been used to characterize flexibility on megahertz and kilohertz timescales in lime fruit cuticle, probing local motional restrictions at polymeric covalent cross-links and cooperative main-chain undulations that may be linked to cuticular resiliency (Garbow and Stark, 1990). In addition, two-dimensional ^1H-^{13}C wide-line separation (WISE) NMR has revealed a population of flexible chain-methylene groups within suberin, a heavily cross-linked aliphatic-aromatic polyester that protects wounded potato tissue from infection (Yan and Stark, 1998). In the present work, both of these solid-state NMR methods have been applied to the cuticle of tomato, chosen because the relative simplicity of its chemical composition constrains the possible molecular origins of its dynamic properties. When combined with AFM studies of tomato cutin conducted under equivalent conditions, these studies allow us to propose a molecular mechanism for the observed changes in cuticular compliance with increasing water content.

MATERIALS AND METHODS

Isolation of cutin

Organically grown tomato fruit cuticles were isolated enzymatically following standard procedures (Pacchiano et al., 1993). Briefly, cuticular samples were removed in large sections (~1–2 cm^2) and soaked in high purity deionized water (EASYpure RF, 18.2 MΩ·cm, Barnstead; Dubuque, IA) for 30 min. Separation of the cuticle from the underlying epidermal fruit tissue was carried out using established procedures by shaking for 2 days at 44°C in 0.4 mg/ml *Aspergillus niger* cellulase (ICN Biomedicals, Aurora, OH) in an acetate buffer (50 mM, pH 5), followed by 5 days at 31°C in 4 mg/ml *A. niger* pectinase (Sigma Chemical Co., Milwaukee, WI) and 1 mM NaN_3 (Sigma Chemical Co.) in an acetate buffer (50 mM, pH 4). Complete removal of cuticular lipids was carried out by successive 2-day Soxhlet extractions at 80°C with methanol, methylene chloride, and tetrahydrofuran. This exhaustive treatment removes both surface-bound epicuticular lipids and interstitial lipids embedded within the insoluble cutin support, but does not alter the chemical structure of the biopolymer (Walton, 1990; Pacchiano et al., 1993). After preparation, the cuticles were dried at room temperature to remove any absorbed solvent before imaging or spectroscopy experiments. Weight loss measurements for the dried samples were made after Soxhlet extraction to assess the degree of lipid removal, which was typically 5–6 wt % and consistent with other studies of lipid content in fruit cuticle (Garbow and Stark, 1990; Petracek and Bukovac, 1995). The isolated cutin was then stored at room temperature in desiccated condition.

Thermal analysis of water content in cutin

The water content of cutin samples prepared under different humidities was measured by thermal gravimetric analysis (TGA) on a TGA 2950 analyzer (DuPont Instruments, Wilmington, DE). Approximately 1 to 2 mg of cutin material was sealed inside a sample pan and heated at 5°C/min from 25°C to 125°C. The experiment was repeated 3 times for each value of humidity (2%, 30%, and 60%) and for samples soaked in high purity water. For the soaked samples, residual surface water was carefully removed by blotting.

NMR spectroscopy

Solid-state NMR spectra were acquired on a Varian (Palo Alto, CA) UNITY*plus* spectrometer operating at a ^1H frequency of 300.001 MHz and a ^{13}C frequency of 75.445 MHz. Experiments were conducted on 30-mg samples of tomato cutin in a Doty 5-mm XC-5 MAS probe at room temperature. Rotor inserts were used to maintain the humidity level in the samples. A Varian speed controller was utilized to maintain a rotor spinning speed of 8000 ± 5 Hz. The ^{13}C chemical shifts were referenced to tetramethylsilane via hexamethylbenzene as a secondary substitution reference. The 90° pulses for ^1H and ^{13}C were both set to 5.0 μs, and a cross-polarization contact time of 500 μs was utilized. Measurements of the ^{13}C signal remaining after a spin-lock of 0.025 to 8.2 ms after cross-polarization from ^1H to ^{13}C were used to derive values of the rotating-frame spin relaxation times $T_{1\rho}(C)$, using only the initial exponential decay between 0 and 0.8 ms to obtain an average value (Schaefer and Stejskal, 1979). Each experiment required about 3 h to complete. The ^{13}C WISE experiments were performed using a previously developed pulse sequence (Schmidt-Rohr et al., 1992; Schmidt-Rohr and Spiess, 1994; Yan and Stark, 1998). The data matrix contained 64 points in the t_1 (^1H) dimension and 1568 points in the t_2 (^{13}C) dimension, which were zero-filled to 1024 and 2048 points, respectively, before two-dimensional Fourier transformation. Spectral widths were set to 100 and 26 kHz in the t_1 and t_2 dimensions, respectively. A recycle delay of 1.5 s was inserted between successive data acquisitions, and a typical WISE experiment lasted 6 h.

Force microscopy

AFM experiments were conducted with a Topometrix Explorer stand-alone atomic force microscope with ECU-Plus electronics (ThermoMicroscopes, Sunnyvale, CA). After drying, the cuticle samples (~1 cm^2) were attached to a Si(100) wafer with double stick tape. Images were collected under controlled conditions in an environmental chamber under 2%, 30%, and 60% (±2%) relative humidity and under high purity water. In each case the sample was allowed to equilibrate for at least 1 h before imaging or NMR

spectroscopy experiments were carried out. Similar experimental results were obtained for samples equilibrated for varying time periods up to several days. The experiments employed commercially available cantilevers (ThermoMicroscopes) with nominal force constants of ~0.37 N/m. The normal force constants of the levers were determined to be 0.36 ± 0.08 N/m based on measurements of the cantilever spring constants against a standardized lever of known spring constant (Tortonese and Kirk, 1997). The tips employed had pyramidal structures with an approximate 1:1 aspect ratio as determined by scanning electron microscopy (AMRAY 1800; KLA-Tencor, San Jose, CA). The proximal tip shape and radius of curvature were determined by imaging of a $SrTiO_3$(305) single crystal that has been shown to yield reliable profiles of AFM tips (Sheiko et al., 1993; Carpick et al., 1996; Ogletree et al., 1996). Tip profiles were obtained in an environmental chamber under dry air conditions (relative humidity <1%) and were routinely found to exhibit a radius of curvature of 53 ± 20 nm. Images were collected in contact mode (contact force of up to 10 nN) with scan sizes between 2 and 80 μm^2 at typical scan rates of 0.25 Hz. Sequential imaging of the same areas over these load ranges confirmed that no permanent damage was done to the surfaces from imaging in contact.

Nanomechanical measurements were conducted on cutin and on a Si(100) single crystal wafer cleaned and oxidized in a 4:1:1 solution of water, NH_4OH, and 30% H_2O_2 (Aldrich, Milwaukee, WI), used as a standard in the point spectroscopy mode. In this mode, the tip is pressed against the sample until a preset force is detected, at which point it is retracted. Each force-distance curve contains 500 data points over a 1000-nm range and is the average of 50 approach-retract cycles at a rate of 1 μm/s. At least 20 force-distance plots were collected randomly over a sample, with no systematic difference detected between various topographical regions (ridges or cellular depressions) of the cutin surface, and each set repeated 5 times for each different condition. The slopes of the force-versus-distance plots during retraction for the indentation of the tip into the cutin and silicon were then used to estimate the Young's modulus of elasticity of the cutin by applying a Hertzian contact mechanics model. All measurements were made at room temperature (22 ± 5°C).

Continuum contact mechanics: the Hertz model

The Hertz model of contact mechanics (Hertz, 1882) was the first attempt to provide a theoretical basis for the physics of contacts between solids. Although it has been extended and refined, most notably by Johnson, Kendall, and Roberts (JKR) and Derjaguin, Muller, and Toporov (DMT) (Israelachvili, 1985; Johnson, 1985), the Hertz model remains a useful and simple method for estimating some of the properties of materials during contact. In particular, it does not account for either short-range (modeled by JKR) or long-range (modeled by DMT) pre-contact attractive interactions, which may cause deformation of one or other of the surfaces in contact. The Hertz model has proven sufficient for modeling of AFM data on soft biological samples (Laney et al., 1997). Its use is favored here by the fact that it does not require prior knowledge of parameters like surface energy, which are difficult to measure accurately for the kinds of (often microheterogeneous) surfaces common in biological systems.

In the current application, the force-distance plots of cutin and silicon, an ideally hard reference, are compared in order to determine the indentation, δ, of the tip into the cutin at a given force. The indentation at a given force is defined as the depth of penetration of the tip into the sample surface. It is calculated with reference to an ideally hard surface, in this case silicon, where the indentation is set at 0.

The indentation is related to the surface area A of the contact between a conical tip of radius R and a flat sample by the following equation:

$$A = 2\pi R\delta$$

The contact area is also related to K, the combined elastic modulus of tip and sample by a second equation:

$$A = \pi\left(\frac{RL}{K}\right)^{2/3} \tag{2}$$

where L = load (nN), the force as measured by the AFM. Thus, we can produce a relationship between K and δ:

$$K = \frac{L}{(8\delta^3 R)^{1/2}} \tag{3}$$

and, because the combined elastic modulus contains the elastic moduli of the tip and sample, we may obtain an expression including E_c, the Young's modulus of elasticity for cutin:

$$K = \frac{4}{3}\left(\frac{1-\nu_t^2}{E_t} + \frac{1-\nu_c^2}{E_c}\right)^{-1} \tag{4}$$

where ν = Poisson ratio and the subscripts t and c refer to the tip and the cutin, respectively. The values of ν_t and E_t are known; in any case, since $E_t \gg E_c$ and we can approximate $E_t = \infty$, the first bracketed term of Eq. 4 reduces to zero, giving:

$$E_c = \frac{3K(1-\nu_c^2)}{4} \tag{5}$$

The value of ν_c is assumed to be similar to that of a polymer such as polystyrene, for which $\nu \cong 0.33$ (Schrader, 1999) and is in the middle of the typical range of values for polymers (0.2–0.5). The radius of the AFM tip was measured from images of a strontium titanate crystal, which possesses nanometer-scale ridges sharp enough to provide a profile of the tip (Sheiko et al., 1993). The same tip was used to obtain force-distance

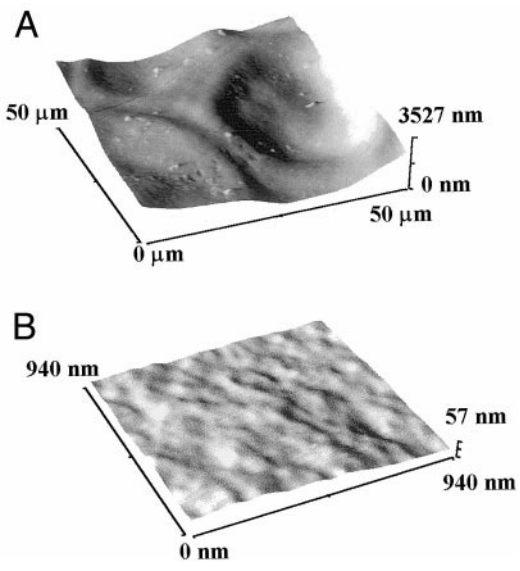

FIGURE 1 (*a*) Three-dimensional topographic image of dewaxed tomato cuticle surface, 50 μm × 50 μm, obtained in water. The image depicts an amorphous material whose contours follow those of the imprints left in the cutin from the removed underlying cells. The height difference between the top ridge of a cell edge and the bottom of the cell depression is approximately 1.4 μm. (*b*) A nanoscale image (940 × 940 nm) of cutin showing the amorphous fibrous nature of the cutin surface.

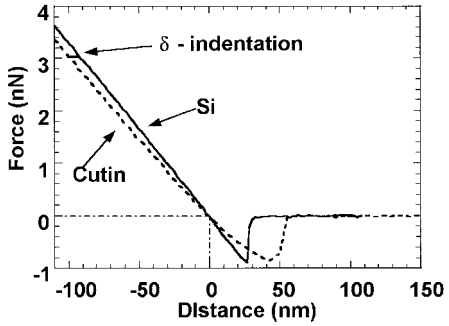

FIGURE 2 Typical force-distance plots showing the indentation of cutin with respect to an ideally hard Si(100) substrate obtained under water, where 0 indentation is defined at 0 force.

plots on cutin and silicon. Measurements taken from over 40 tips produced an average value of $R = 53 \pm 20$ nm, which is used in the calculation.

RESULTS AND DISCUSSION

Nanorheological studies

Before performing each nanoindentation experiment, the surface of the cutin was imaged. The images clearly show the outline of the impressions left in the cutin where the underlying plant cells once resided (Fig. 1 *a*). At least 20 force-distance curves were collected at random from within 10 μm^2 areas in each sample, with no systematic difference detected between various topographical regions of the cutin surface (i.e., no differences observed for data collected on the ridges of the cellular outlines versus those collected within the depressions). High-resolution images of the cutin surface (Fig. 1 *b*) show an amorphous surface structure with roughness on the order of ~8 nm rms. No structural changes are observed for the isolated cutin surface structure for any of the degrees of hydration studied. The sample was then translated to expose the underlying silicon wafer support and force-distance data collected there as well.

The average gradients of the retract curves on cutin and silicon were calculated for each set of data at a load of 3 nN, and the indentation depth (δ) was obtained at this load (Fig. 2). This indentation value varied from ~1 to 9 nm from the lowest to highest degree of cutin hydration, respectively. Applying the Hertzian formalism outlined above, the relationship between Young's elastic modulus and humidity was deduced (Fig. 3 *a*). This plot shows a clear trend of decreasing elastic modulus with increasing water exposure, dropping from an average of ~32 MPa under the driest environment to ~6 MPa when the sample is saturated with water. The sharp decrease in elastic modulus is nearly complete upon exposure of the sample to a 60% relative humidity environment, suggesting that little water uptake is required to modify the surface modulus. Interestingly, although the bulk response to the uptake of water by the cutin (Fig. 3 *b*) shows the same net decrease in elasticity (about fivefold), the bulk shows a strikingly different near-linear trend in its response to water uptake as compared to the highly nonlinear response of the surface deduced by AFM. The details of these bulk elasticity experiments are being described elsewhere (manuscript in preparation).

By taking the results from thermal analysis into account, it is possible to re-express the surface elasticity trends in terms of the water content of the cutin (Fig. 4). Here we see that the change in modulus results from the absorption of very modest amounts of water, and that an increase in water content of only ~1 to 2 wt % above the driest conditions yields the observed precipitous drop in modulus. These elastic modulus results indicate the biopolymer cutin behaves as a rubbery polymer and that the water functions as a plasticizer within the polymer matrix, reducing the chain-chain interactions within the polymer and increasing overall chain mobility (Jelinski et al., 1985; Schaefer et al., 1987). The fact that the modulus shows no further decrease, even under water-soaked conditions, suggests that upon the uptake of 2 to 3 wt % water, the near surface region has already been saturated, and that no further changes in elasticity are detectable by AFM.

Molecular-level dynamic profile

The CPMAS ^{13}C NMR spectrum of dry tomato cutin is shown in Fig. 5, along with spectral assignments derived from prior work on lime fruit cutin (Zlotnik-Mazori and Stark, 1988). In order to complement the nanorheological studies described above and develop a molecular picture of

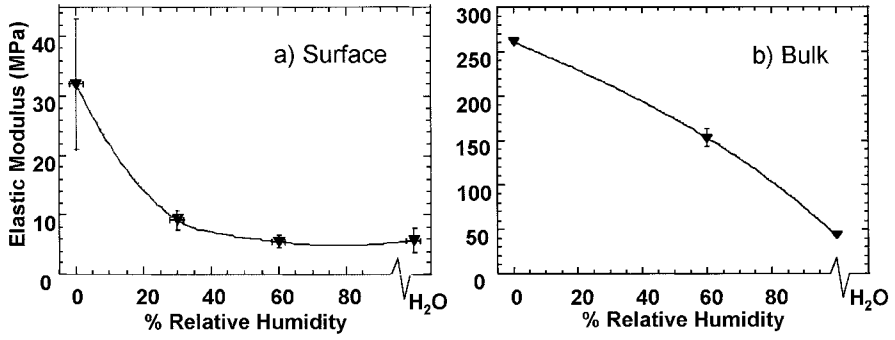

FIGURE 3 Graphs showing (*a*) the decrease in surface elastic modulus with increasing humidity from dry to ambient conditions determined by AFM and (*b*) the decrease in the bulk elastic modulus measured from conventional rheometry.

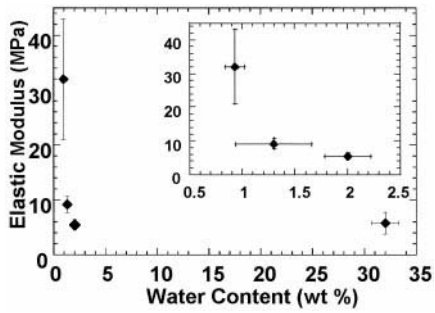

FIGURE 4 Reiteration of Fig. 3 *a*, substituting the water content values (wt %) of the cuticle under the humidity conditions described. The inset shows the rapid decrease in surface elastic modulus with only a small increase in the amount of water present.

the changes in cuticle surface elasticity that accompany water absorption, a series of rotating-frame ^{13}C NMR spin relaxation experiments was conducted in parallel with the AFM measurements. Table 1 summarizes the average relaxation times observed for two major functional groups in tomato cutin: methylene carbons of the aliphatic chains and oxygenated carbons near covalent cross-links and/or hydrogen-bonding sites of the biopolyester. These times reflect cooperative main-chain undulations at frequencies close to 50 kHz, which may be associated in turn with bulk polymer rheological properties such as impact strength (Schaefer and Stejskal, 1979; Garbow and Stark, 1990). As in prior NMR studies of lime cutin (Garbow and Stark, 1990), the shorter values of $\langle T_{1\rho}(C)\rangle$, and thus the more efficient motions in the mid-kHz frequency regime, are observed for the $(CH_2)_n$ groups of tomato cutin's long acyl chains rather than for its oxymethine groups. Nonetheless, the values of $\langle T_{1\rho}(C)\rangle$ at *C*HOCOR carbons are five times shorter than observed for analogous functional groups in engineering polymers such as butyral derivatives of poly(vinyl alcohol) (Schaefer et al., 1987). Table 1 shows that these NMR relaxation times are not altered significantly by modest degrees of water uptake;

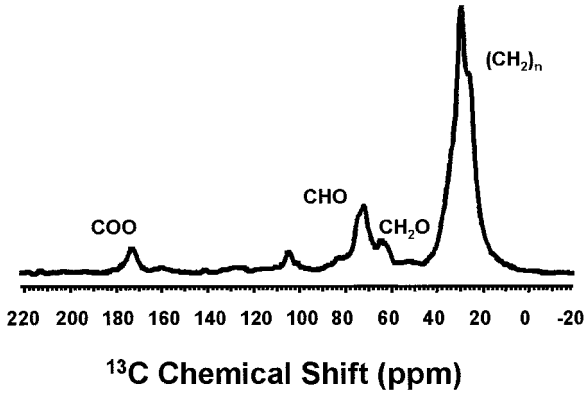

FIGURE 5 75-MHz CPMAS ^{13}C NMR spectrum of dry tomato cutin, showing resonances from the principal carbon moieties in the biopolyester. Chemical shifts are referenced to tetramethylsilane, as described in the text.

TABLE 1 Rotating-frame ^{13}C NMR relaxation parameters for carbons in tomato cuticle

	$\langle T_{1\rho}(C)\rangle$ (ms)	
Avg. wt% water	$(CH_2)_n$	*C*HOCOR, CHOH
0.9	2.3 ± 0.1	5.5 ± 1.0
1.3	2.7 ± 0.2	5.2 ± 1.6
2.0	2.8 ± 0.2	5.8 ± 1.5
32.0	2.0 ± 0.1	3.1 ± 0.3

Data were derived from the short-time behavior (0.05–0.80 ms) of ^{13}C magnetization held in a 50-kHz radiofrequency field after spin locking and cross-polarization from ^{1}H. The uncertainties on the spin-relaxation parameters are reported as the first standard deviation of the data.

they are shortened only upon saturation of the cutin samples with water and then primarily at the cross-link sites.

Secondly, two-dimensional ^{1}H-^{13}C WISE was used to probe the degree of motional averaging experienced for protons attached to particular carbon types within the cutin polymer. Unlike measurements of the relaxation time $T_{1\rho}(H)$, which report the average mid-kHz motions for a solid material, ^{1}H powder patterns in the traces of a 2D WISE spectrum are sensitive to faster molecular dynamics and can detect separate rigid and mobile spin populations that correspond to each magnetically inequivalent ^{13}C site (Schmidt-Rohr et al., 1992). The spectrum of dry tomato cutin displays two $(CH_2)_n$ resonances of differing breadth: a 5-kHz component attributable to relatively mobile chain segments and a 35-kHz component that may arise from rigidly bound methylene groups in close proximity to the covalent cross-links within the cutin network (Fig. 6). In addition to the $(CH_2)_n$ resonances, a broader ^{1}H lineshape indicative of molecular rigidity is observed for the CHOCOR moieties. A similar distribution of WISE lineshapes has been reported for the suberin plant polyester synthesized in wounded potato tissue (Yan and Stark, 1998).

In contrast to the $T_{1\rho}(C)$-based picture of mid-kHz dynamics, tomato cutin motions exceeding ~50 kHz become progressively more prevalent in more humid environments, as indicated by the decreasing $(CH_2)_n$ linewidths and increasing proportion of the narrow ^{1}H spectral component (Table 2). These linewidths reflect local reorientation of the acyl chain segments, which have been associated with the modulus, i.e., resistance to deformation, of a polymeric material (Ledwith and North, 1975). Although limitations in signal sensitivity preclude examination of analogous trends for the CHO groups, it is notable that gains in the efficiency of rapid segmental motions are evident even for bulk-methylene groups remote from the polymeric covalent cross-links. The increasing percentage of $(CH_2)_n$ groups with motionally averaged ^{1}H linewidths (~5 kHz) that accompanies hydration of the tomato cutin samples also suggests an overall shift in the spectral density of motions toward faster local dynamic processes and more flexible carbon segments.

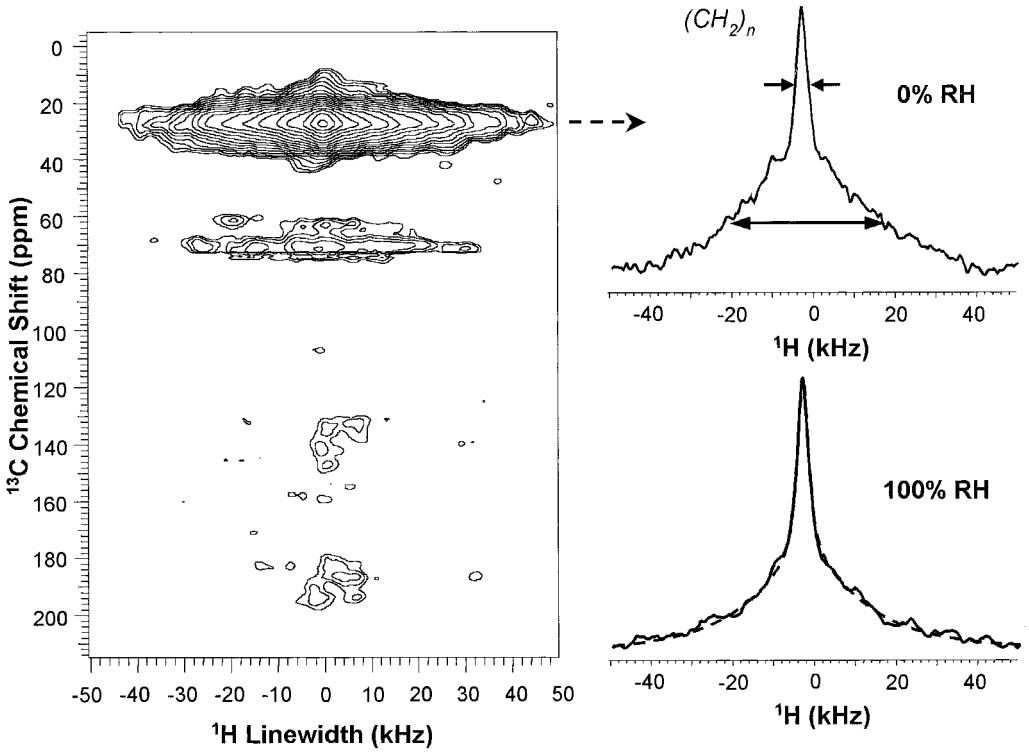

FIGURE 6 Contour plot (*left*) and ^{1}H spectral slices (*right*) from ^{1}H-^{13}C 2D WISE spectra of dry tomato cutin. The proton powder pattern corresponding to the bulk-methylene carbons consists of overlapping broad and narrow peaks, with estimated linewidths of 35 and 5 kHz, respectively. A ^{1}H spectral slice of tomato cutin soaked with water is also shown for comparison, along with dashed lines showing the spectral simulation described in Table 2.

CONCLUSION

The coordinated use of AFM, TGA, and NMR methodologies suggests the following molecular picture of the influence of water content on the mechanical properties of the cutin biopolymer. Water absorbed by the cutin functions as a plasticizer, promoting molecular flexibility that softens the polymer network and thus decreases its elastic modulus. This phenomenon could occur if water disrupts hydrogen-bonded cross-links between chains and diminishes existing chain-chain hydrophobic interactions. These changes permit enhanced local reorientation of the chain methylene groups (reflected experimentally in the ^{1}H lineshapes derived from WISE NMR), but evidently no changes in slow overall dynamics (as judged from the constancy of $\langle T_{1\rho}(C)\rangle$). In turn, dramatic changes in the surface and bulk elastic modulus are expected and observed as a consequence of hydration-induced changes in these rapid local motions. The predominance of 10,16-dihydroxyhexadecanoic acid monomers in tomato cutin (Gerard et al., 1992) provides only limited hydrogen bonded cross-linking possibilities, allowing even modest levels of water absorption to exert a dramatic influence on flexibility and elasticity as observed. The fact that AFM-based changes in modulus are reflected only in $T_{1\rho}(C)$ relaxation times for the water-saturated samples suggests that cuticular water uptake occurs predominantly at the surface region, which is monitored more sensitively by AFM than NMR of bulk samples. The rapid drop-off in modulus observed by AFM is a result of the near surface region being completely disrupted by water at a relative humidity of 60%, whereas the bulk elasticity has only declined by a factor of two under these conditions. Our AFM and NMR studies offer complementary views of nanomechanics and molecular mobility, respectively, opening the door to further investigation of the rheological changes associated with foliar surfactants that can alter

TABLE 2 NMR-Derived flexibility of bulk-methylene groups in tomato cuticle

	^{1}H Linewidth		
Avg. wt% water	Broad component (kHz)	Narrow component (kHz)	% Narrow component*
0.9	38.2	5.3	9
1.3	36.2	5.7	12
2.0	32.3	4.9	12
32.0	31.3	4.7	18

Data were derived from two-dimensional ^{1}H-^{13}C WISE NMR measurements of motionally averaged ^{1}H spectral patterns corresponding to the designated carbon signals resonating at 30 ppm. The CHO carbons absorbing at 72 ppm had corresponding ^{1}H linewidths of 40–50 kHz.

*From spectral deconvolution of narrow and broad components of the chain-methylene resonance; estimated uncertainties are 20%.

cuticular permeability. A detailed comparative study of bulk and surface rheology, as well as the impact of the cuticular lipids on the cuticle's dynamic response, is forthcoming.

We gratefully acknowledge support of this work by the U.S. Department of Agriculture National Research Initiative (grant 97–35106-4800), the National Science Foundation (NSF grant MCB-9728503), and the PSC-CUNY Research Awards Program of The City University of New York (grants 67599 and 69324). S. D. was supported by the Research Experience for Undergraduates Program of the NSF and the Dean's Summer Research Program at City University of New York-College of Staten Island. R. E. was supported by the NSF-CUNY Alliance for Minority Participation Program. J. D. B. also acknowledges support via a collaborative agreement with ThermoMicroscopes.

We thank Professor William L'Amoreaux, Department of Biology, City University of New York-College of Staten Island, for assistance in obtaining scanning electron microscopy images of our AFM tips.

REFERENCES

Agrios, G. N. 1988. Plant Pathology. Academic Press, New York.

Baker, E. A. 1982. Chemistry and morphology of plant epicuticular waxes. *In* The Plant Cuticle. D. F. Cutler, K. L. Alvin and C. E. Price, editors. Academic Press, New York. 139–165.

Canet, D., R. Rohr, A. Chamel, and F. Guillain. 1996. Atomic force microscopy study of isolated ivy leaf cuticles observed directly and after embedding in epon. *New Phytol.* 134:571–577.

Domke, J., and M. Radmacher. 1998. Investigation of the mechanical properties of thin polymeric films. *Langmuir.* 14:3320–3325.

Carpick, R. W., N. Agrait, D. F. Ogletree, and M. Salmeron. 1996. Measurement of interfacial shear (friction) with an ultrahigh vacuum atomic force microscope. *J. Vac. Sci. Tech. B.* 14:1289–1295.

Garbow, J. R., and R. E. Stark. 1990. Nuclear magnetic resonance relaxation studies of plant polyester dynamics. 1. Cutin from limes. *Macromolecules.* 23:2814–2819.

Gerard, H. C., S. F. Osman, W. F. Fett, and R. Moreau. 1992. Separation, identification and quantification of monomers from cutin polymers by high-performance liquid chromatography and evaporative light-scattering detection. *Phytochem. Anal.* 3:139–144.

Gould, S. A. C., B. Drake, C. B. Prater, A. L. Weisenhorn, S. Manne, G. L. Kelderman, H. J. Butt, H. Hansma, and P. K. Hansma. 1990. The atomic force microscope: a tool for science and industry. *Ultramicroscopy.* 33:93–98.

Gracias, D. H., and G. A. Somorjai. 1998. Continuum force microscopy study of the elastic modulus, hardness and friction of polyethylene and polypropylene surfaces. *Macromolecules.* 31:1269–1276.

Hertz, H. 1882. Über die Berührung Fester Elasticher Körper. *J. Reine Angew. Mathematik.* 92:156–171.

Holloway, P. J. 1982. Structure and histochemistry of plant cuticular membranes: an overview. *In* The Plant Cuticle. D. F. Cutler, K. L. Alvin, and C. E. Price, editors. Academic Press, New York. 1–32.

Israelachvili, J. N. 1985. Intermolecular and Surface Forces. Academic Press, London.

Jelinski, L. W., J. J. Dumais, A. L. Cholli, T. S. Ellis, and F. E. Karasz. 1985. Nature of the water-epoxy interaction. *Macromolecules.* 18: 1091–1095.

Johnson, K. L. 1985. Contact Mechanics. Cambridge University Press, London.

Kirby, A. R., A. P. Gunning, K. W. Waldron, V. J. Morris, and A. Ng. 1996. Visualization of plant cell walls by atomic force microscopy. *Biophys. J.* 70:1138–1143.

Kiridena, W., V. Jain, and G.-Y. Liu. 1997. Nanometer-scale elasticity measurements on organic monolayers using force microscopy. *Surface Interface Anal.* 25:383–389.

Kolattukudy, P. E. 1984. Biochemistry and function of cutin and suberin. *Can. J. Bot.* 62:2918–2933.

Kolattukudy, P. E. 1980. Biopolyester membranes of plants: cutin and suberin. *Science.* 208:990–1000.

Laney, D. E., R. A. Garcia, S. M. Parsons, and H. G. Hansma. 1997. Changes in the elastic properties of cholinergic synaptic vesicles as measured by atomic force microscopy. *Biophys. J.* 72:806–813.

Ledwith, A., and A. M. North, eds. 1975. Molecular Behavior and the Development of Polymeric Materials. Chapman and Hall, London.

Mechaber, W. L., D. B. Marchall, R. A. Mechaber, R. T. Jobe, and F. S. Chew. 1996. Mapping leaf surface landscapes. *Proc. Natl. Acad. Sci. USA.* 93:4600–4603.

Overney, R. M., E. Meyer, J. Frommer, H.-J. Güntherodt, M. Fujihira, H. Takano, and Y. Gotoh. 1994. Force microscopy study of friction and elastic compliance of phase-separated organic thin films. *Langmiur.* 10:1281–1286.

Ogletree, D. F., R. W. Carpick, and M. Salmeron. 1996. Calibration of frictional forces in atomic force microscopy. *Rev. Sci. Instrum.* 67: 3298–3306.

Pacchiano, R. A., W. Sohn, V. L. Chlanda, J. R. Garbow, and R. E. Stark. 1993. Isolation and spectral characterization of plant cuticle polyesters. *J. Agric. Food Chem.* 41:78–83.

Petracek, P. D., and M. J. Bukovac. 1995. Rheological properties of enzymatically isolated tomato fruit cuticle. *Plant Physiol.* 109:675–679.

Radmacher, M., R. W. Tillmann, M. Fritz, and H. E. Gaub. 1992. From molecules to cells, imaging soft samples with the atomic force microscope. *Science.* 257:1900–1905.

Round, A. N., A. R. Kirby, and V. J. Morris. 1996. Collection and processing of AFM images of plant cell walls. *Microsc. Anal.* Sept.: 33–35.

Schaefer, J., J. R. Garbow, E. O. Stejskal, and J. A. Lefelar. 1987. Plasticization of Poly(butyral-*co*-vinyl alcohol). *Macromolecules.* 20: 1271–1278.

Schaefer, J., and E. O. Stejskal. 1979. High-resolution ^{13}C NMR of solid polymers. *Top. Carbon-13 NMR Spectrosc.* 3:283–324.

Schmidt-Rohr, K., J. Clauss, and H. W. Spiess. 1992. Mobility and morphological information in heterogeneous polymer materials by two-dimensional wideline-separation NMR spectroscopy. *Macromolecules.* 25:3273–3277.

Schmidt-Rohr, K., and H. W. Spiess. 1994. Multidimensional Solid-State NMR and Polymers. Academic Press, London.

Schrader, D. 1999. Physical constants of poly(styrene). *In* Polymer Handbook, 4th edition. J. Brandrup, E. H. Immergut, and E. A. Grulke, editors. Wiley Interscience, New York. V/91-V/96.

Sheiko, S. S., M. Möller, E. M. C. M. Reuvekamp, and H. W. Zandbergen. 1993. Calibration and evaluation of scanning-force microscopy probes. *Phys. Rev. B.* 48:5675–5678.

Tortonese, M., and M. Kirk. 1997. Characterization of application specific probes for SPMs. *SPIE Proc.* 3009:53–60.

Walton, T. J. 1990. Waxes, cutin and suberin. *Methods Plant Biochem.* 4:105–158.

Yan, B., and R. E. Stark. 1998. A WISE NMR approach to heterogeneous biopolymer mixtures: dynamics and domains in wounded potato tissues. *Macromolecules.* 31:2600–2605.

Zlotnik-Mazori, T., and R. E. Stark. 1988. Nuclear magnetic resonance studies of cutin, an insoluble plant polyester. *Macromolecules.* 21: 2412–2417.